Performance of concretes manufactured with newly developed low-clinker cements exposed to water and chlorides: characterization by means of electrical impedance measurements

G. Cosoli[1], A. Mobili[2], N. Giulietti[1], P. Chiariotti[1], G. Pandarese[1], F. Tittarelli[2,3], T. Bellezze[2], N. Mikanovic[4], G. M. Revel[1]

[1]*Department of Industrial Engineering and Mathematical Science (DIISM), Università Politecnica delle Marche, 60131, Ancona, Italy.*

[2]*Department of Materials, Environmental Sciences and Urban Planning (SIMAU), Università Politecnica delle Marche – INSTM Research Unit, 60131, Ancona, Italy.*

[3]*Institute of Atmospheric Sciences and Climate, National Research Council (ISAC-CNR), Via Gobetti 101, 40129 Bologna, Italy.*

[4]*Global R&D, HeidelbergCement AG, Oberklamweg 2-4, 69181, Leimen, Germany.*

Corresponding author: Tel.: +39 071 220 4976

E-mail address: p.chiariotti@univpm.it (Paolo Chiariotti).

Highlights

- Electrical impedance is used as NDT for concrete health status assessment
- Three concrete compositions were subjected to accelerated degradation tests
- Wenner's method is used for measuring electrical impedance in AC configuration
- Electrical impedance decreases with water/chlorides penetration
- Low-clinker cements help in increasing detectability of aggressive agents

Abstract

This paper discusses the electrical impedance behaviour, measured according to the Wenner's method, of three different concrete mixes during accelerated degradation tests. Being a first attempt to move from laboratory to in-field applications targeted to long-term monitoring, the same electrode

array configuration and set-up (AC current at 10kHz) is used. Results show that electrical impedance decreases down to 24% in capillary water absorption tests, 77% and 86% in salt-spray chamber and wet/dry cycles with 3.5% NaCl solution, respectively. The two new low-clinker cements adopted seem to improve the measurement sensitivity towards contaminants ingress with respect to the commercial one (reference).

Keywords

Electrical impedance measurement, Concrete, Durability, Concrete Health Monitoring

1. Introduction

Concrete durability is a key aspect to consider in structures (buildings, tunnels, bridges, etc.), since it highly affects their service life costs. The durability of concrete heavily depends on the interactions of concrete itself with the surrounding environment, which is reach in contaminants [1]. Indeed, among the several causes of concrete degradation, the following three are considered as the most common ones:

- Water penetration, which represents the main carrier of aggressive agents;
- CO_2 penetration, which, in presence of moist air, determines cement matrix carbonation, responsible of reinforcements corrosion;
- Chloride penetration, both through water and marine aerosol, which initiates reinforcements corrosion;

From “The law of fives” by De Sitter, it is well known that costs for repairing a concrete structure exponentially grow with the time elapsed from the first sign of degradation to the intervention [2]. Consequently, it becomes clear that monitoring the penetration of aggressive agents in concrete to speed up interventions is important to reduce maintenance costs and avoid premature failure of concrete structures [3]. Several non-destructive measurement techniques for static Structural Health Monitoring (SHM) are reported in literature, such as ultrasound [4,5], Ground Penetrating Radar

(GPR) [6,7], electrical resistivity [8], computer vision [9] and thermography [10,11]. Electrical resistivity measurement, which can be calculated from electrical impedance (i.e. the ability of a material to oppose the electric current flow), is getting high attention with respect to the other methods, given its low-cost nature and fast response. Indeed, the electrical impedance characteristics make it possible to exploit self-sensing capability of concrete, which means its ability to sense its own condition (e.g. damage, temperature variations, stress and strain) [12]. Since concrete contains an interstitial solution with ions, conduction is of electrolytic type; however, in presence of conductive materials (e.g. carbon fibres) also electric conduction occurs [13]. It is possible to state that electrical resistivity reflects the ability to transport ions [14] (e.g. chlorides and sulphates [15]) and therefore the concrete capability to withstand the mobility of ions [8], which are directly involved in degradation processes.

To measure electric impedance, the material under test should be excited (by means of an electric current/potential) and the corresponding response (in terms of potential difference/electric current, respectively) should be measured. The ratio between electric potential and current provides an electric impedance value.

Electrodes needed to perform this measurement should be in contact with the material under investigation; indeed, a good electrical connection is fundamental to get reliable measurements [16]. To guarantee the absence of polarization of both electrodes and the material itself, the measurement should be carried out adopting the Alternating Current (AC) approach in the 4 electrodes configuration (i.e. Wenner's method [17]). Literature reports valid examples of different approaches (e.g. AC 2-electrode configuration [20,21], Direct Current [22,23] to cite some) providing interesting results, however, it should be noted that the 4-electrodes AC configuration, makes it possible to improve the accuracy of the measurement process, for the following reasons [18,19]:

- Exciting the material with AC prevents material polarization, since dipoles have not enough time to align; even though this could be material dependent, frequency should be > 1 kHz, otherwise a small polarization could still be present;

- As it is common in electric impedance measurements, carrying out a 4-electrode measurement reduce insertion errors; measurement electrodes are separated from the excitation ones and the inner input electric impedance of the device carrying out the measurement does have a reduced impact on the characterization of the target electric impedance to be tested.

Electrical resistivity (ρ [Ω·m]) is widely used to characterize concrete for different aspects, such as corrosion of reinforcement steel rebars [19,25,26] (also resistivity ranges with associated corrosion risks are reported in literature [8]), assuming that higher resistivity entails slower corrosion propagation [27–29]), cracks detection [4,30–32], setting-time determination [13,14], resistance to chloride penetration [33], moisture content, porosity [34–36], quality assessment and, therefore, durability of concrete itself [8,37,38]. In particular, it is possible to observe a decrease of concrete electrical resistivity if moisture content increases (moisture is the main factor influencing resistivity [14]), as well as chloride content (strong correlation, $R^2 > 0.90$ [33]), if total porosity is higher (which means presence of more pore solution) or temperature increases (which entails higher ionic mobility) [8]. On the other hand, electrical resistivity increases after cement matrix carbonation (which reduces interstitial fluid ion concentrations), cracks [30,39], high tortuosity (i.e. small and disconnected pores), high concrete age (indeed, hydration increases pores discontinuity). It makes little sense to establish electrical impedance ranges for normal concrete conditions, since intrinsic impedance value depends on concrete composition [14,21] (i.e. on the electrical conductivity and electrical permittivity [6] of the used materials, e.g. aggregates [40], binders [37], conductive additions) and curing conditions [41], in addition to the influence of the measurement method itself [42–44]. This means that each type of concrete should be characterized in its initial condition before monitoring of its health status. Moreover, the cell-constant of the specimen under test has to be known [45,46]. Cell-constant of laboratory specimens can be determined; obtaining the cell constant in in-field applications is not practical, since the extension of the structure with respect to the material volume

under analysis might highly affect the accuracy in the determination of the cell-constant, thus causing high uncertainty in the resistivity value.

It is worthy to underline that Wenner's method makes it possible to monitor a limited volume (which is referred to as "sensing volume"), i.e. the hemisphere whose radius is equal to the electrodes spacing, hence it is a local measurement. If a change in electric impedance takes place outside this monitored volume, the measurement will not be affected. For this reason, it is fundamental to install the required amount of sensors in a given structure through a suitable strategy for the selection of the zones that play a key role in the mechanical resistance of the structure in relation to their critical exposure conditions to aggressive environments.

Literature already reports papers where electric impedance/resistivity has been used to monitor the penetration of contaminants in concrete [33,47]. However, generally, a single type of aggressive agent has been considered. Moreover, different measurement configurations (in terms of number of electrodes, measured frequency, etc.) and different mixtures have been adopted by different authors; this makes very difficult the comparison of the obtained results.

This paper aims at developing a long-term monitoring system for concrete-based structures. For this reason, a comprehensive set of concrete specimens were manufactured and submitted to accelerated degradation tests (capillary water absorption, exposure to a salt-spray chamber and exposure to wet-dry cycles in a chloride-rich solution, simulating sea water). The concrete specimens were analysed in terms of electric impedance measurements by means of the same 4 electrode array configuration (4 electrode array) and electrical input (AC approach, 10 kHz excitation frequency). Given the increasing interest in low-clinker cement for reducing cement carbon footprint (Ordinary Portland Cement (OPC) production generates around 8% of global CO_2 emissions [48]), the investigation was performed on concrete specimens adopting new formulations of low-clinker cement developed within the framework of the EnDurCrete (GA No. 760639) European Project [49].

Three different concrete compositions have been tested in order to investigate the effect of the binder on the measured electrical impedance in the different (above-mentioned) accelerated degradation tests

and to verify that the measurement itself is not altered by the contaminants. This is fundamental to bring the electrical impedance-based approach from laboratory to the field as a long-term structural health monitoring system.

2. Materials and methods

2.1. Concrete specimens preparation

Three different Portland cements were used as binders for concrete specimens. In particular, two were developed by HeidelbergCement AG within EnDurCrete project (CEM II/C-M (S-LL) and CEM VI (S-V)), whereas a commercially available one was used as reference cement (CEM II/A-S 42.5R):

- CEM II/A-S 42.5R was used to cast specimens belonging to the R0 subset;
- CEM II/C-M (S-LL) was used to cast specimens belonging to the S1 subset; this cement is a blend of ordinary Portland cement, ground granulated blast furnace slag and limestone filler;
- CEM VI (S-V) was used to cast specimens belonging to the S2 subset; this cement is a blend of ordinary Portland cement, ground granulated blast furnace slag and V-type fly ash.

Table 1 Composition [wt%] of CEM II/C-M (S-LL) and CEM VI (S-V) cements

Cement	CEM I 52.5 R	GGBFS	Limestone filler	CEM I 42.5 R	Coarse GGBFS	FA
CEM II/C-M (S-LL)	50	40	10	-	-	-
CEM VI (S-V)	-	-	-	47	43	10

The composition of the two newly developed low-clinker cements is reported in Table 1 and they have been produced by blending OPC component together with separately ground granulated blast furnace slag (GGBFS), limestone filler and fly ash (FA). CEM II/C-M (S-LL) and CEM VI (S-V) contain only 50 wt.% and 47 wt.% of CEM I, respectively, and the European Standardization Committee is currently working on adding these low-clinker cement types to the family of common

cements within the scope of EN 197-1 [50]. The novel cements have been designed and produced by Heidelberg Cement on principles which are described in [51].

Three aggregates were used in saturated surface dry (s.s.d.) condition; in particular, limestone/quartz river sand (0/4 mm) and intermediate (5/10 mm) and coarse (10/15 mm) river gravel. Water absorption was 1.3%, 0.9% and 0.7%, for sand, intermediate and coarse gravel, respectively. The particle size distribution of aggregates is reported in Fig. 1.

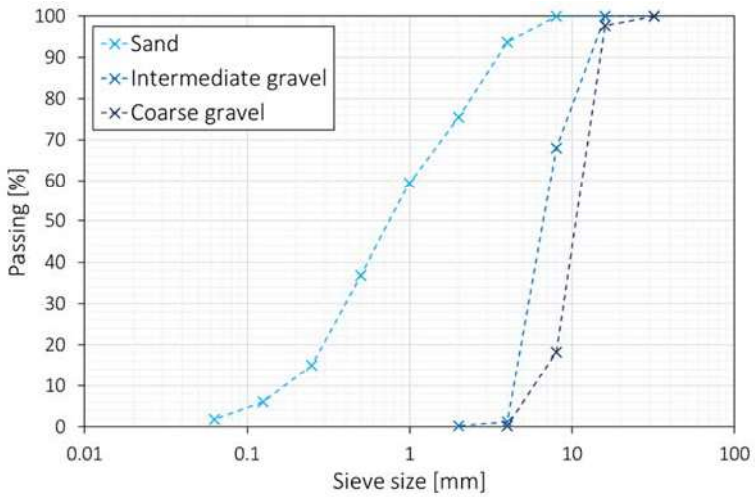

Fig. 1 Particle size distribution of aggregates

Two polycarboxylate (PC)-based admixtures were used: PC1 is a high-range water reducer, specially designed for precast applications, and PC2 is a slump-keeper for obtaining highly fluid concrete, avoiding loss in workability and additional retardation.

Table 2 Mix-design of concrete specimens

Mix	Cement [kg/m^3]	Effective water [kg/m^3]	Sand [kg/m^3]	Intermediate gravel [kg/m^3]	Coarse gravel [kg/m^3]	Admixtures [kg/m^3]	
						PC1	PC2
R0	360	162	956	385	567	1.2	1.9
S1	360	162	953	384	566	1.7	2.5
S2	360	162	956	385	567	0.9	1.3

R0, S1 and S2 concrete subsets were cast with the mix-design reported in Table 2. The admixtures amount was dosed in order to obtain concretes of S5 consistency ("almost Self-Compacting Concrete"), with a water/cement (w/c) ratio equal to 0.45.

The concrete batches were mixed according to the following procedure:

1. Mix solid components: sand + gravel + cement (mix speed: 30 rpm; mixing time: 20 s);
2. Stop the mixer;
3. Add three quarter of water and mix the concrete (mix speed: 59 rpm; mixing time: 60 s);
4. Stop the mixer;
5. Add one quarter of water + PC-based water reducers and mix the concrete (mix speed: 59 rpm; mixing time: 600 s).

PC-based water reducers were added to reach the same workability class (S5).

Fresh concrete mixtures were then poured into different moulds to obtain specimens for testing, namely in 10 cm cubes and 10 cm x 10 cm x 50 cm beams. Curing was performed in a climate chamber at temperature (T) of 20 ± 1 °C and a relative humidity (RH) of 95 ± 5% by covering specimens with plastic film for the first 24 hours; then, they were demoulded and wrapped in polyethylene foils for further 27 days. Then, the plastic envelopes were removed and specimens were left at T = 20 ± 1 °C and RH = 50 ± 5% before being exposed to accelerated degradation tests.

2.2. Porosimetry testing

The microstructural properties of the concretes, in terms of pore distribution and total porosity (V_p) value, were analysed after 28 days of curing by means of a mercury intrusion porosimeter (MIP, model Thermo Fisher 240 Pascal). It is worthy to note that the pore size that can be measured with this system ranges between 0.0037 μm and 7.5 μm; pores bigger than 7.5 μm cannot be directly measured; however, macropores greater than 1 mm can be observed visually.

2.3. Electrical impedance measurement

After 28 days of curing, the beams were cut in three parts, in order to obtain two smaller prisms (10 cm x 10 cm x 20 cm) and one cube (side: 10 cm). The formers were used for electrical impedance measurements, whose electrodes configuration is reported in Fig. 2. The external electrodes (i.e. Working Electrode, WE, and Counter Electrode, CE) are used to inject excitation current (RMS value: 10 μA), whereas the internal ones (i.e. Sensing, S, and Reference Electrode, RE) are used to measure electric potential difference. Stainless steel electrodes (Ø 3 mm, length 4 cm), with a spacing of 4 cm (that is greater than 1.5 times the maximum aggregate size, as recommended in [19]), were embedded for half of their length (i.e. 2 cm). In particular, they were inserted in holes drilled in concrete (Ø 18 mm, height 20 mm), then filled with mortar, whose composition is reported in Table 3.

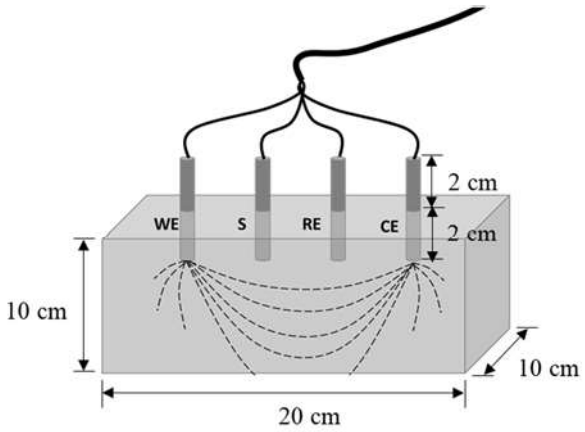

Fig. 2 Concrete specimen with sensing electrodes, dashed lines represent electric current (dimensions are not in scale)

The cement used to cast the mortar was the same used in each concrete composition: CEM II/A-S 42.5R for R0, CEM II/C-M (S-LL) for S1 and CEM VI (S-V) for S2. Limestone filler, with particle size smaller than 100 μm, produced by Granulati Vertova S.r.l. (Rezzato, BS, Italy), was used. An acrylic ether superplasticizer (Dynamon SP1) was used as admixture. Calcium oxide (CaO) was used to avoid possible shrinkage phenomena. The mortar was cast with a w/c equal to 0.67.

Table 3 Mix-design of the mortar used to fill holes

Cement [kg/m^3]	Water [kg/m^3]	Limestone filler [kg/m^3]	Dynamon SP1 [kg/m^3]	CaO [kg/m^3]
467	311	1400	3.1	23.3

Table 4 reports the number of specimens per each composition manufactured for the different accelerated degradation tests.

Table 4 No. of concrete specimens for each accelerated degradation test

Accelerated test	Subset	Specimens	
		Cubic shape (10 cm × 10 cm × 10 cm)	Parallelepiped shape (10 cm × 10 cm × 50 cm)
Capillary water absorption	R0	-	1
	S1	-	1
	S2	-	1
Chloride penetration (wet/dry cycles)	R0	1	1
	S1	1	1
	S2	1	1
Salt-spray chamber	R0	1	1
	S1	1	1
	S2	1	1

Measurements were carried out according to the Electrochemical Impedance Spectroscopy (EIS) method, in the frequency range 10 Hz – 100 kHz (then, the electrical impedance measured at different single frequency values, i.e. 1, 10, 31.6, 50.2 and 100 kHz, were derived), by means of Gamry Reference 600 Potentiostat/Galvanostat, used in galvanostatic configuration. Single frequency values were extracted in post-processing, to evaluate the variations of electrical impedance while

contaminants penetrate; in particular, the real part of electrical impedance was taken into account, since it is the one mostly related to concrete durability (indeed, it is linked to the ions mobility in concrete pore solution) [43]. Results reported in the Section 3 refer to the analysis frequency of 10 kHz. This frequency was chosen as it seems to provide good balance between the ability to detect changes in the material electrical impedance due to contaminants and measurement speed. Indeed, these two aspects are important in terms of development of an in-field monitoring system, since a fast measurement makes it possible to reduce consumption of the data acquisition system and to evaluate the response of the target structure to transient phenomena like dynamic load variations. Nevertheless, the use of an EIS approach should be kept, if possible, also in an in-field monitoring system, for timely check of the performance of both the target structure and the measurement system itself.

2.4. Capillary water absorption

Capillary water absorption test was carried by adapting the EN 15801 [52] conditions to electrical impedance measurement (specimens were not dried in the oven to avoid extremely high impedance values, beyond the instrumentation full-scale). Distilled water was used to soak 1-cm multilayer of filter paper. Specimens were placed over the paper in vertical position, as shown in Fig. 3a. Specimens were kept in a closed container for all the test duration, in order to avoid water evaporation (Fig. 3b). According to the above-mentioned standard, the specimen weights were periodically measured over time to evaluate the amount of water absorbed per unit area (Q_i [kg/m^2]).

Both weighing and electrical impedance measurements were carried out at 0 (start of test, after 28 days of curing), 10, 20, 30 and 60 minutes, 4, 6, 24, 48, 72, 144, and 168 hours.

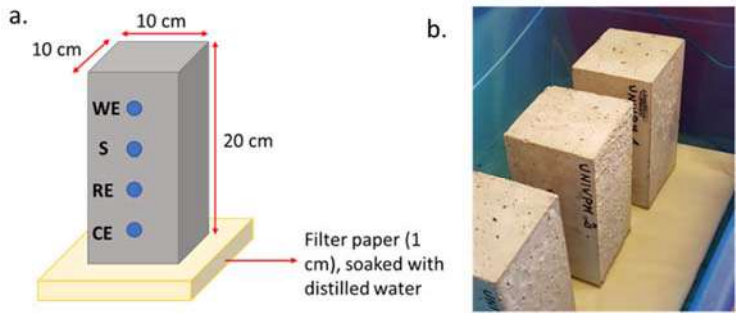

Fig. 3 Capillary water absorption test setup: a. sketch with dimensions and b. picture

2.5. Salt-spray chamber exposure

Salt-spray chamber test was carried out according to EN ISO 9227 [53] in warm, humid and chloride-rich environment (T = 38 ± 2 °C, RH = 95-98%, NaCl = 5%). Specimens were placed inside the salt-spray chamber (ACS DCTC 600 P) on proper supports, as illustrated in Fig. 4. To prevent possible corrosion of electrodes, these were sealed with plasticine. Measurements were carried out after a preliminary 28-day exposure in the chamber, in order to start with specimens having an initial degradation level.

Fig. 4 Salt-spray chamber test setup

Free chlorides (i.e. water soluble chlorides) have been measured because directly related to reinforcement pitting corrosion [3,54]. Free chloride concentration was analysed in compliance to UNI 9944 [55]; powder samples were drilled (Fig. 5) from cubic specimens (side: 10 cm) having exactly the same composition and curing conditions/time and exposed to the same conditions of those

with the electrodes used for impedance measurements. The set times for electrical impedance measurement were 0, 7, 14, 21 and 28 days, whereas for chloride analyses were 0, 14 and 28 days. Powder samples (approximately 5 g each) were collected drilling the cubes at four different depths: 0-10 mm, 10-20 mm, 20-30 mm and 30-40 mm; contamination between the powders collected at the different depths was avoided by cleaning the holes with compressed air. Each collected powder sample was mixed with 20 ml of demineralized water. The obtained suspension was maintained under a strong mixing for 24 hours and then filtered to obtain a final solution in a 100 ml volumetric flask by adding the necessary demineralized water. The free chloride content was determined as wt.% of the cement.

Fig. 5 Drilling of powder samples for free chloride analysis

2.6. Chloride penetration (wet/dry cycles)

To carry out a wet-dry cyclic exposure of the concrete specimens, they were submitted to 4 weekly wet/dry cycles (2 days wet and 5 days dry) in a 3.5% NaCl solution. They were partial immersed (constant depth: 9 cm) in the solution. In order to allow water penetration also from the bottom side of the specimens, they were placed inside a closed plastic box on cylindrical supports (Fig. 6).

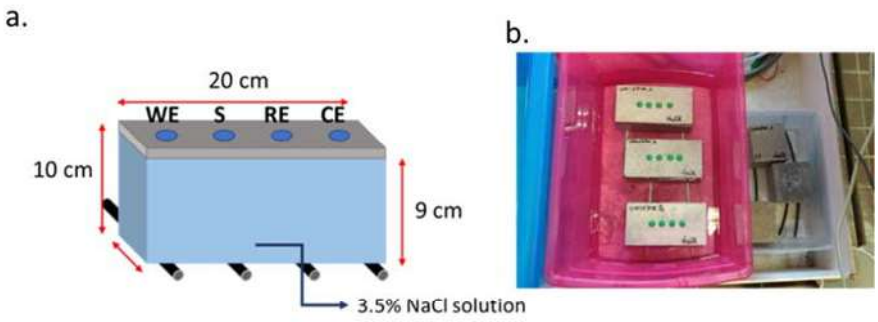

Fig. 6 Chloride penetration (wet/dry cycles) test setup: a. sketch with dimensions and b. picture

As for salt-spray chamber test, the electrodes were sealed with plasticine to prevent possible corrosion.

The free chlorides concentration in the specimens as a function of depth was analysed in compliance to UNI 9944 [55], as described in the previous section. This analysis was always performed on cubic specimens submitted to the same exposure program of the specimens with electrodes. Electric impedance tests were carried out both in wet (i.e. at the end of immersion) and dry (i.e. at the end of the dry period, immediately before the next immersion) conditions (i.e. 0, 2, 7, 9, 14, 16, 21, 23 and 28 days). Chloride analyses were performed at times of 0, 9 and 23 days.

All concrete specimens had undergone 3 wet/dry cycles in order to start measurements with specimens having an initial degradation level.

3. Results and discussion

3.1. Porosimetry testing

Results in terms of total porosity (V_p) are reported in Table 5, whereas the pore distribution is shown in Fig. 7. It is possible to observe that the reference concrete (R0) and that manufactured with the novel cement CEM VI/S-V (S2) have comparable porosity, equal to 9%, whereas S1 concrete is the least porous, with a V_p equal to 7%. However, all the tested compositions show very low total porosity values; this was predictable if considering that tests are performed on concrete with relatively low

w/c, equal to 0.45, and the measurement range involving pores smaller than 7.5 μm. As it is possible to observe in Fig. 7, both R0 and S1 have the highest percentage of pores around 0.2 and 0.1 μm, respectively, whereas S2 concrete shows the highest concentration of pores in two different ranges, centred at approximately 0.01 μm and 0.1 μm. This porosity is generally associated with gel-like hydrates.

Table 5 Porosimetry testing results

Specimen	V_p [%]
R0	9
S1	7
S2	9

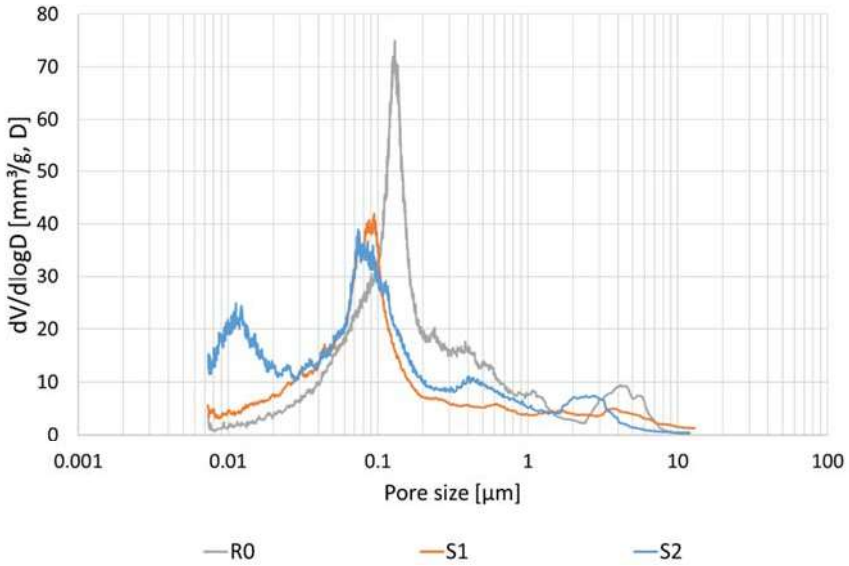

Fig. 7 Pore size distribution measured after 28 days of curing

The macroporosity of the different concretes tested was analysed by visual inspection (Fig. 8); it is possible to observe that S2 shows an increased number of macropores with respect to R0 and S1.

Fig. 8 Visual aspect of concrete specimens: a. R0, b. S1 and c. S2

3.2. Capillary water absorption

Electrical impedance measured at different single frequency values (i.e. 1, 10, 31.6, 50.2 and 100 kHz, derived from EIS measurement settings) gives quite similar trends (Fig. 9). Therefore, the only frequency value of 10 kHz was chosen, as reported in Section 2.1. This choice was the same for all the performed tests. Moreover, for ease of readability, the term "electrical impedance" will be used referring to the real part of electrical impedance (Z_{Re}).

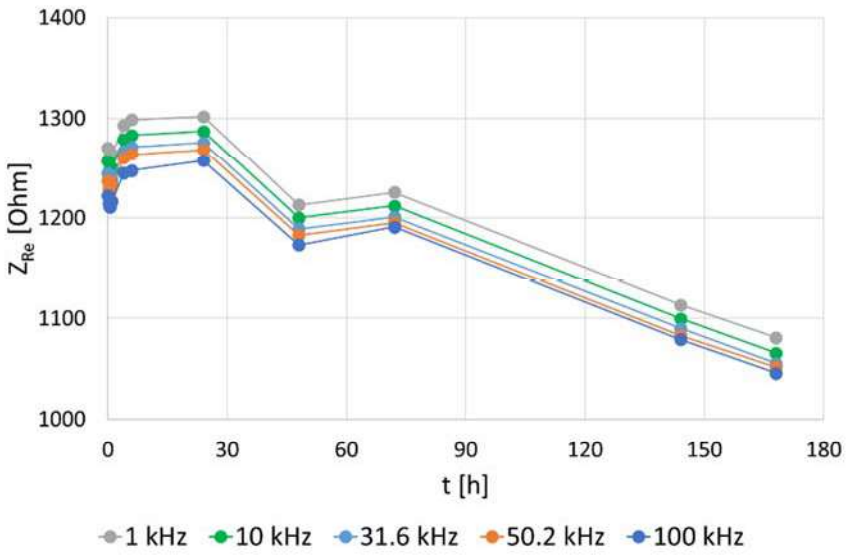

Fig. 9 Results of capillary water absorption: electrical impedance at multiple frequency values (example on R0 specimen)

While water penetrates, electrical impedance decreases, as expected from literature results [56]; the maximum decrease values are equal to approximately -14%, -15% and -24% for S1, R0 and S2,

respectively, in correspondence of a Q_i equal to 1.39, 2.00 and 2.35 kg/m^2 (measured at the end of the test), respectively. However, the measurement of electrical impedance does not seem to be influenced by water penetration.

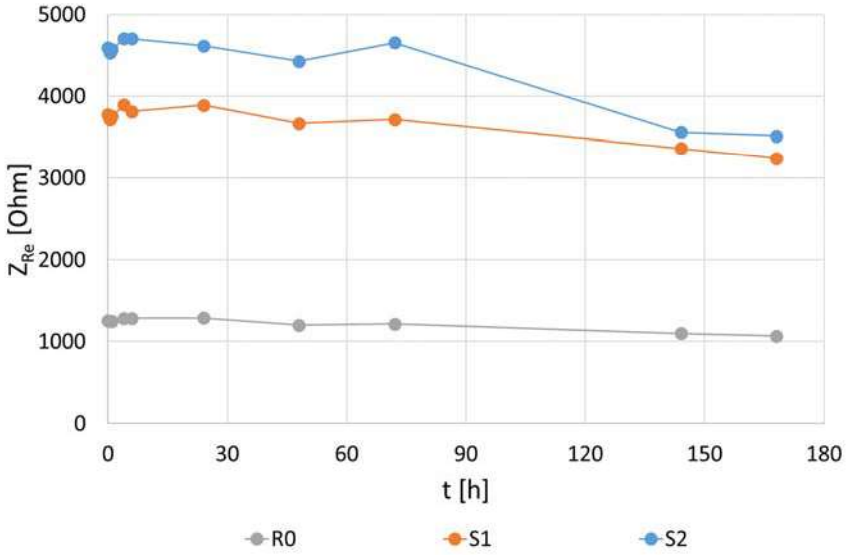

Fig. 10 Results of capillary water absorption test: electrical impedance (at 10 kHz) over test time

The amount of absorbed water increases over time: S2 is the specimen absorbing the most one, followed by R0 and S1. In general, water absorption depends on porosity which is linked to concrete microstructure (pores size, connectivity and tortuosity) [57]. In particular, the higher the porosity, the greater the permeability and the lower the concrete durability, since aggressive agents can penetrate more easily. In fact, the concrete with the lowest porosity (S1, Table 5 and Fig. 8) is the one which absorbs less water. On the other hand, comparing R0 and S2 concretes, it is possible to state that the latter have a higher amount of macropores, as detected by visual inspection (Fig. 8), hence capillary water absorption takes place in a shorter time [58].

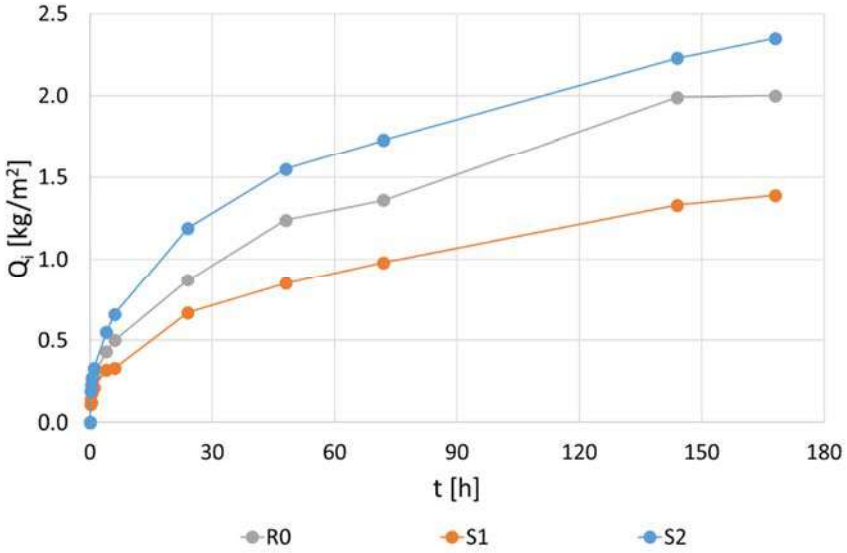

Fig. 11 Results of capillary water absorption test: water absorbed per unit area

Electrical impedance is highly influenced by concrete composition. Indeed, the cement type is probably the most influencing factor in the testing campaign shown in this paper.

Looking at the correlation between electrical impedance (rescaled to the initial value, in order to have 0 y-intercept) and water absorbed per unit area (Fig. 12), it is possible to notice that electrical impedance remains almost constant until water reaches the sensing volume, then it decreases together with water absorption. S2 shows a higher sensitivity, followed by S1 and R0, meaning that innovative cements (i.e. CEM II/C-M (S-LL) and CEM VI (S-V)) provides a positive contribution on self-sensing property of concrete.

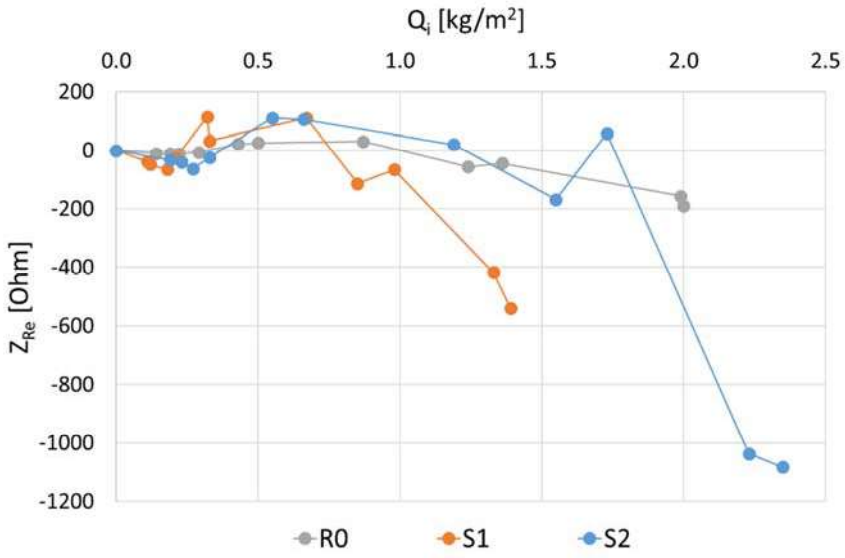

Fig. 12 Correlation between electrical impedance (rescaled to have 0 y-intercept) and water absorbed per unit area

3.3. Salt-spray chamber

Chlorides percentage trends, as a function of penetration depth and exposure time, are reported in Fig. 13 for the three tested compositions. It is possible to observe that already at 0 test time the chloride content is not null, since the concrete specimens had already been subjected to 28 days exposure in salt-spray chamber.

As it was predictable, free chloride concentration decreases with increasing depth. S1 is the specimen showing the lowest free chloride concentration: from capillary water penetration test it is possible to notice that it is the one absorbing the least (Fig. 11), since its porosity is the lowest (Fig. 8b). R0 is the specimen with the higher free chloride concentration: this is due to the higher total porosity than S1 (Table 5), the bigger pore size distribution (Fig. 7) and the lower amount of supplementary cementitious materials (SCMs), namely slag and fly ash, in the used cement. It is well known that SCMs are able to bind a high quantity of chlorides offering a resistance to the penetration of chloride ions [59]. Even if chloride concentration is expected to increase over time, a decrease is observable in the 0-10 mm depth layer, which corresponds to the most external one, of R0 specimen. This could be related to the leaching at the outermost section as leaching phenomena of free chlorides have an impact on chloride ingress profile in concrete [60,61].

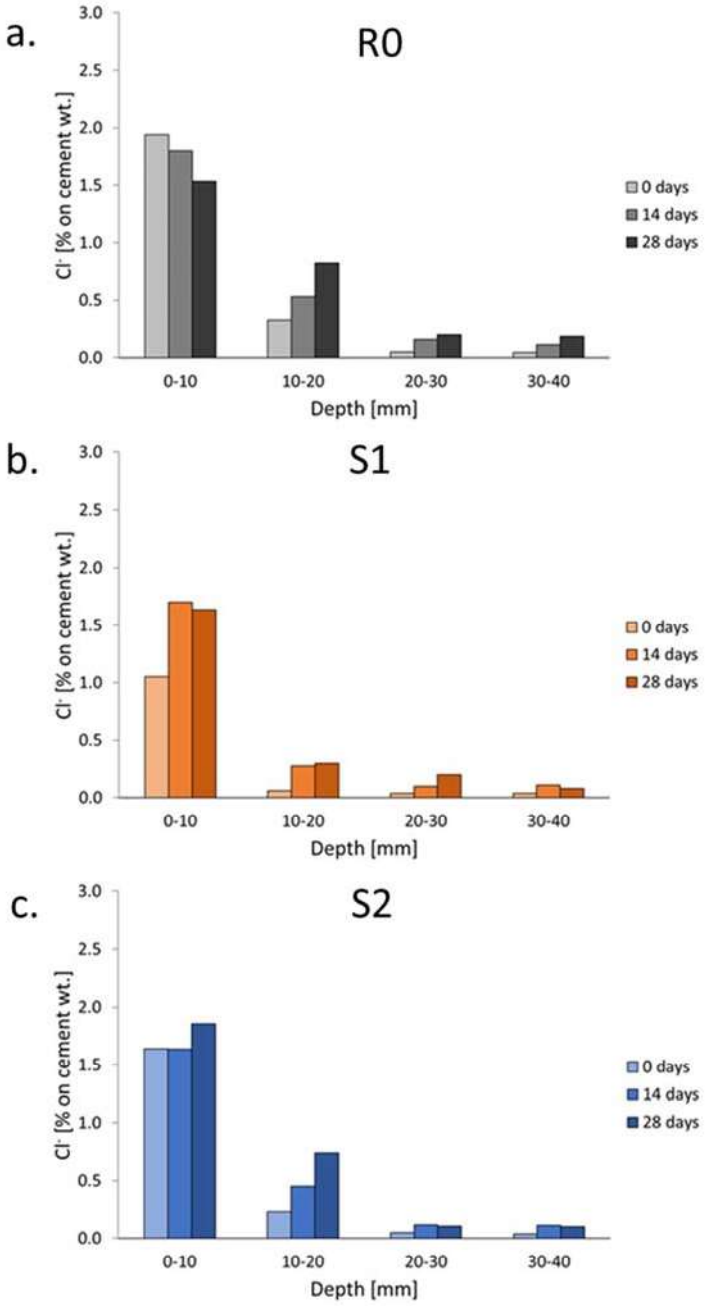

Fig. 13 Free chloride profiles in salt-spray chamber test for the three tested compositions

The average value among the four depths (Fig. 14) was calculated for each testing time in order to evaluate its correlation with electrical impedance. R0 is the only specimen that at 28 days of exposure seems to have reached saturation in chloride penetration, whereas the trend is increasing for both S1 and S2 (Fig. 14). As already stated, SCMs, such as GGBFS, provide to concretes a higher capability to bind chlorides [59], thus slowing down their penetration at the same concrete total porosity.

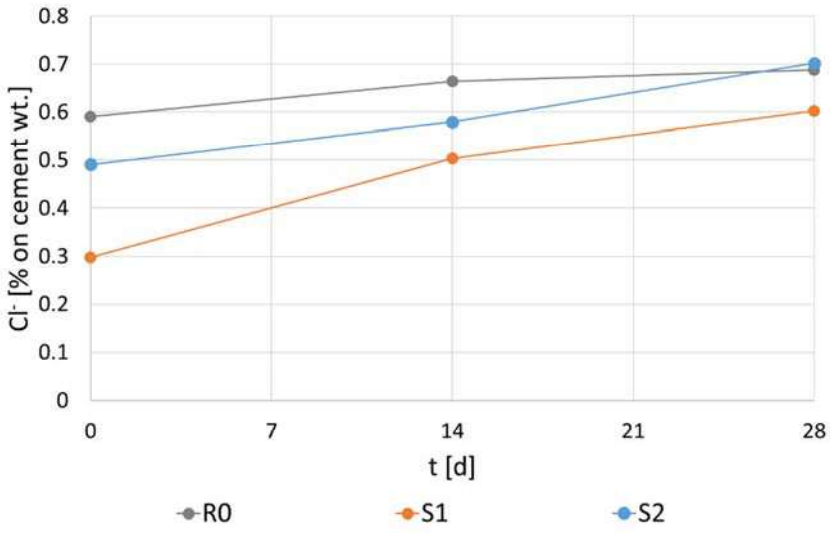

Fig. 14 Results of salt-spray chamber test: free chloride content on cement weight (0-40 mm depth)

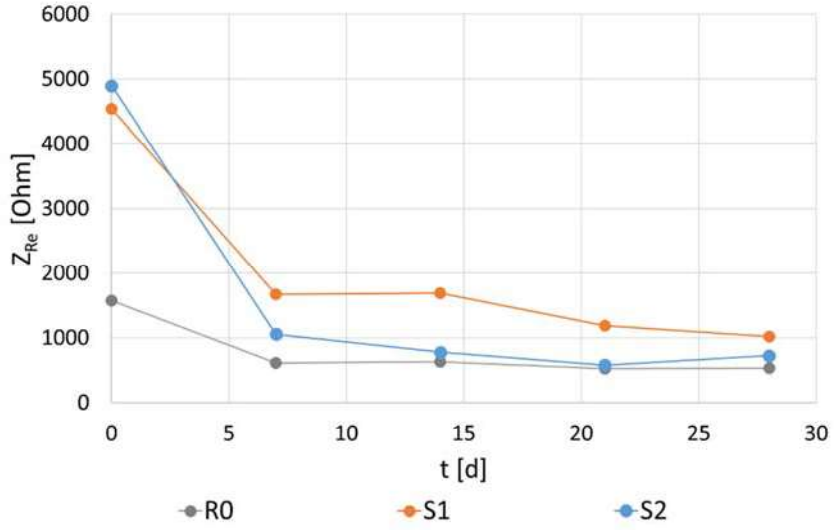

Fig. 15 Results of salt-spray chamber test: electrical impedance (at 10 kHz) over test time

As expected, electrical impedance decreases while chlorides penetrate [15,33,36,56]; the change is more evident in the first week of test, when also water plays a fundamental role in decreasing the electrical resistivity of concrete (Fig. 15). The maximum decrease values are equal to approximately -77%, -66% and -88% for S1, R0 and S2, respectively, in correspondence of a free chloride content on cement weight equal to approximately 0.6%, 0.7% and 0.7%, respectively. It is important to

observe that electrical impedance measurement does not appear to be spoiled by chloride penetration, since results are in line with those reported in literature [15,33,36,56].

The correlation between electrical impedance (rescaled to the initial value, in order to have 0 y-intercept) and free chloride content on cement weight is reported in Fig. 16: S2 shows the highest sensitivity (i.e. the curve slope is higher), followed by S1 and R0.

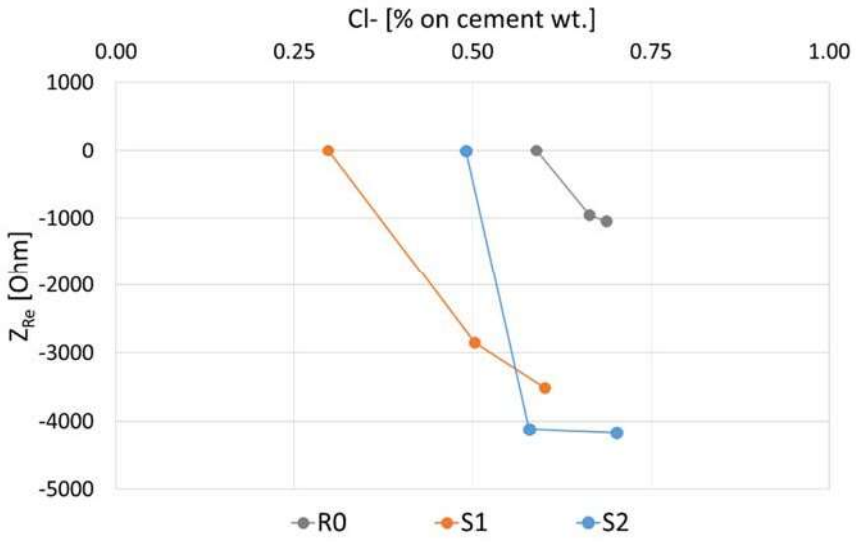

Fig. 16 Correlation between electrical impedance (rescaled to have 0 y-intercept) and free chloride content

3.4. Chloride penetration (wet/dry cycles)

Chlorides profile are reported in Fig. 17 for the three tested compositions. As for salt-spray chamber, the chloride content is not null at the beginning of the test, since the concrete specimens had already been subjected to 3 wet/dry cycles.

Chloride concentration decreases with increasing depth; S2 is the specimen with the highest chloride penetration, in fact during capillary water penetration test (Fig. 18) it is the one absorbing the most.

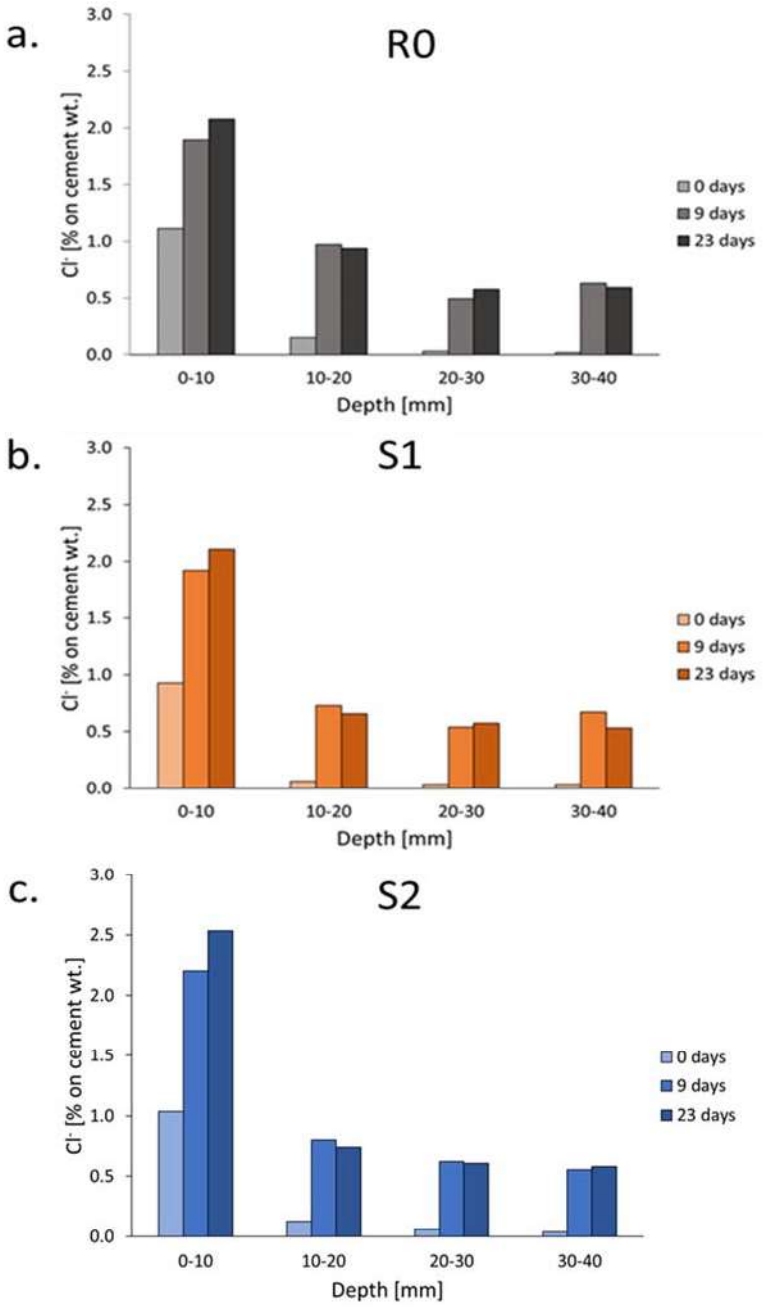

Fig. 17 Free chloride profiles in chloride penetration test for the three tested compositions

As for salt-spray chamber test, to correlate electrical impedance results with chloride penetration, the average chloride content among the four depths (Fig. 19) was calculated for each testing time. As expected, chlorides penetration generally causes a decrease of electrical impedance [15,33,36,56].

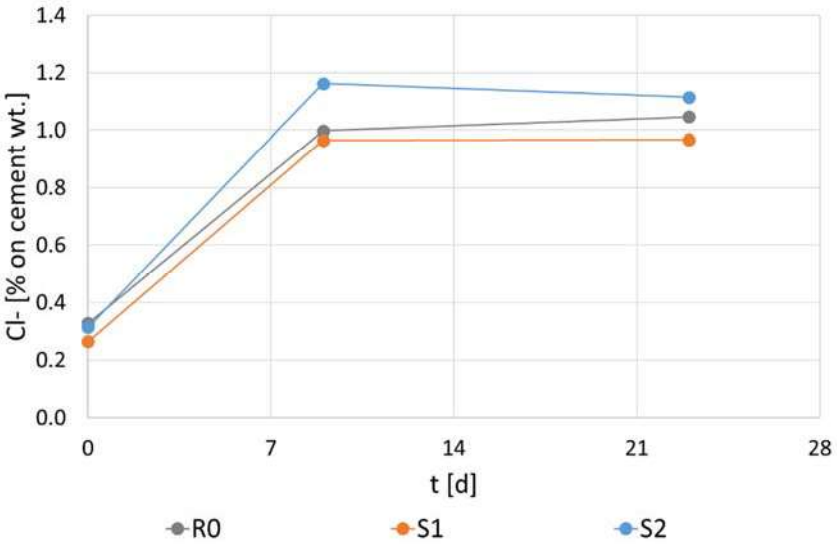

Fig. 18 Results of chloride penetration test: free chloride content on cement weight

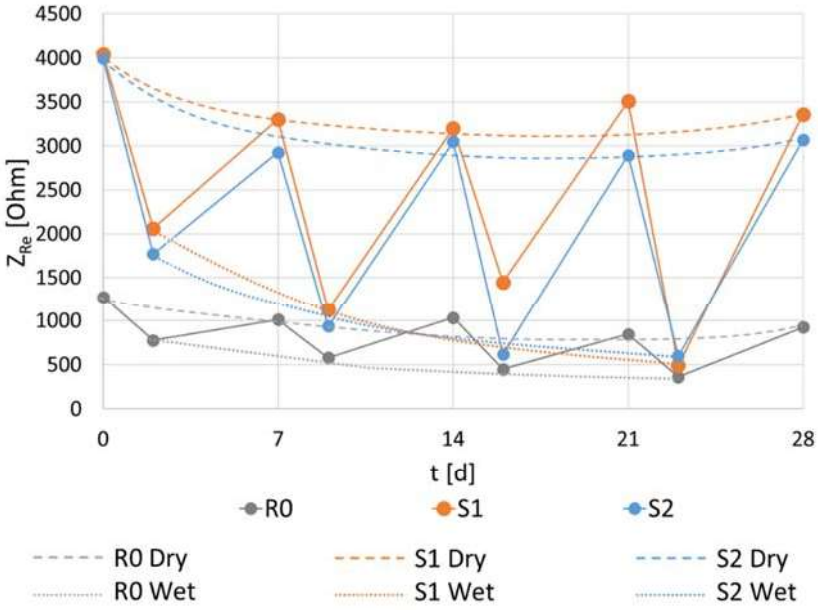

Fig. 19 Results of chloride penetration test: electrical impedance (at 10 kHz) over test time

Electrical impedance measurement follows the trend of wet/dry cycles; in particular, electrical impedance decreases in wet condition, whereas it increases when specimen is dry (Fig. 19). Both wet and dry specimens show decreasing trends in electrical impedance, since chlorides decrease concrete electrical resistivity. The maximum decrease values are equal to approximately -86%, -57% and -

82% for S1, R0 and S2, respectively, in correspondence of a free chloride content on cement weight equal to approximately 1.0%.

The correlation between electrical impedance (rescaled to the initial value, in order to have 0 y-intercept) and free chloride content on cement weight is reported in Fig. 20; it is possible to notice that correlations are better in dry conditions, in which there is no contribution of water.

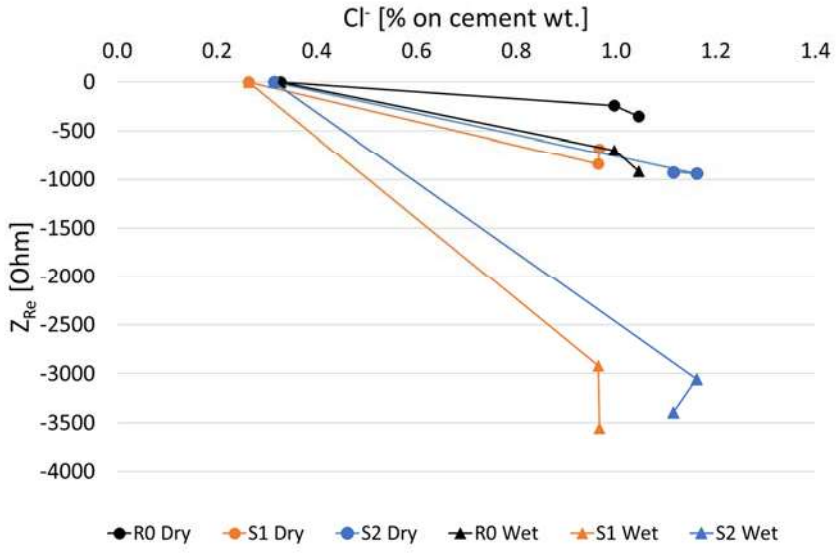

Fig. 20 Correlation between electrical impedance (rescaled to have 0 y-intercept) and free chloride content

4. Conclusions

This paper has presented a first attempt to move the Wenner's impedance-based approach for checking the health status of concrete from laboratory to in-field applications targeted to long-term monitoring of structures. To understand the feasibility of this transfer, a series of accelerated degradation tests, namely capillary water absorption, exposure to salt-spray chamber and chloride penetration by wet-dry cycles in a chloride solution, have been performed on three different concrete mixes with the same electrode array configuration, as well as the same electric configuration of the impedance test, AC current at 10 kHz.

The electrical impedance measurement configuration adopted has proved to be suitable for concrete monitoring both during capillary water absorption and chloride penetration; in fact, the measurement of electrical impedance does not seem to be spoiled by the penetration of these contaminants. A decrease in electrical impedance is observed in case of penetration of both chloride and water. The two cements CEM II/C-M (S-LL) and CEM VI (S-V) seem to provide higher sensitivity of electrical impedance towards water and chloride penetration.

It is worthy to note that authors have chosen to consider electrical impedance real part and not electrical resistivity because this is transferrable to in-field applications more easily (no need to consider cell-constant).

Results obtained show that S1 concrete, manufactured with CEM II/C-M (S-LL), has the best performance: a low penetration of water and chlorides has been registered; this can be due to the reduced porosity with respect to the other concretes tested.

It is worthy to note that the adopted configuration is suitable mainly for laboratory testing; authors are currently performing further studies with electrodes, embedded in the concrete structure during its casting phase, targeted to long-term monitoring. Indeed, in this perspective, it is important to avoid any air-exposed conductive element, as it could represent preferable path for aggressive agents.

Acknowledgements

This research activity was carried out within the EnDurCrete (New Environmental friendly and Durable conCrete, integrating industrial by-products and hybrid systems, for civil, industrial and offshore applications) project, funded by the European Union's Horizon 2020 research and innovation programme under grant agreement n° 760639. Authors would like to thank ACCIONA group for having prepared concrete specimens to be tested, NTS and SIKA for having provided aggregates and admixtures, respectively.

References

[1] M. Sufian Badar, K. Kupwade-Patil, S.A. Bernal, J.L. Provis, E.N. Allouche, Corrosion of steel bars induced by accelerated carbonation in low and high calcium fly ash geopolymer concretes, Constr. Build. Mater. 61 (2014) 79–89. https://doi.org/10.1016/j.conbuildmat.2014.03.015.

[2] W.R. de Sitter, Costs of service life optimization "The Law of Fives," (1984) 131–134.

[3] L. Bertolini, B. Elsener, P. Pedeferri, R. Polder, Corrosion of Steel in Concrete: Prevention, Diagnosis, Repair, Wiley Blackwell, Weinheim, 2005. https://doi.org/10.1002/3527603379.

[4] M. Goueygou, O. Abraham, J.F. Lataste, A comparative study of two non-destructive testing methods to assess near-surface mechanical damage in concrete structures, NDT E Int. 41 (2008) 448–456. https://doi.org/10.1016/j.ndteint.2008.03.001.

[5] S. Ould Naffa, M. Goueygou, B. Piwakowski, F. Buyle-Bodin, Detection of chemical damage in concrete using ultrasound, in: Ultrasonics, 2002: pp. 247–251. https://doi.org/10.1016/S0041-624X(02)00146-4.

[6] X. Dérobert, G. Villain, Effect of water and chloride contents and carbonation on the electromagnetic characterization of concretes on the GPR frequency band through designs of experiment, NDT E Int. 92 (2017) 187–198. https://doi.org/10.1016/j.ndteint.2017.09.001.

[7] J. Hugenschmidt, R. Mastrangelo, GPR inspection of concrete bridges, Cem. Concr. Compos. 28 (2006) 384–392. https://doi.org/10.1016/j.cemconcomp.2006.02.016.

[8] P. Azarsa, R. Gupta, Electrical Resistivity of Concrete for Durability Evaluation: A Review, Adv. Mater. Sci. Eng. 2017 (2017). https://doi.org/10.1155/2017/8453095.

[9] D. Feng, M.Q. Feng, Computer vision for SHM of civil infrastructure: From dynamic response measurement to damage detection – A review, Eng. Struct. 156 (2018) 105–117. https://doi.org/10.1016/j.engstruct.2017.11.018.

[10] Y. Jia, L. Tang, P. Ming, Y. Xie, Ultrasound-excited thermography for detecting microcracks in concrete materials, NDT E Int. 101 (2019) 62–71. https://doi.org/10.1016/j.ndteint.2018.10.006.

[11] P. Cotič, D. Kolarič, V.B. Bosiljkov, V. Bosiljkov, Z. Jagličić, Determination of the applicability and limits of void and delamination detection in concrete structures using infrared thermography, NDT E Int. 74 (2015) 87–93. https://doi.org/10.1016/j.ndteint.2015.05.003.

[12] D.D.L. Chung, Carbon materials for structural self-sensing, electromagnetic shielding and thermal interfacing, Carbon N. Y. 50 (2012) 3342–3353. https://doi.org/10.1016/j.carbon.2012.01.031.

[13] J. Donnini, T. Bellezze, V. Corinaldesi, Mechanical, electrical and self-sensing properties of cementitious mortars containing short carbon fibers, J. Build. Eng. 20 (2018) 8–14. https://doi.org/10.1016/j.jobe.2018.06.011.

[14] K. Osterminski, R.B. Polder, P. Schießl, Long term behaviour of the resistivity of concrete, Heron. 57 (2012) 211–230. https://repository.tudelft.nl/islandora/object/uuid%3Ac77effc5-c5bd-46db-813e-bcc4fb5efa54.

[15] M. Saleem, M. Shameem, S.E. Hussain, M. Maslehuddin, Effect of moisture, chloride and sulphate contamination on the electrical resistivity of Portland cement concrete, Constr. Build. Mater. 10 (1996) 209–214. https://doi.org/10.1016/0950-0618(95)00078-X.

[16] A.J. Ewins, Resistivity measurements in concrete, Br. J. Non-Destructive Test. 32 (1990) 120–126.

[17] F. Wenner, A method for measuring Earth resistivity, J. Washingt. Acad. Sci. 5 (1915) 561–563. https://www.jstor.org/stable/24520849.

[18] T.-C. Hou, Wireless and Electromechanical Approaches for Strain Sensing and Crack Detection in Fiber Reinforced Cementitious Materials, University of Michigan, 2008.

[19] K.R. Gowers, S.G. Millard, Measurement of Concrete Resistivity for Assessment of Corrosion Severity of Steel Using Wenner Technique, Mater. J. 96 (1999) 536–541. https://doi.org/10.14359/655.

[20] S. Feliu, C. Andrade, J.A. González, C. Alonso, A new method forin-situ measurement of

electrical resistivity of reinforced concrete, Mater. Struct. 29 (1996) 362–365. https://doi.org/10.1007/BF02486344.

[21] T.C. Hou, V.K. Nguyen, Y.M. Su, Y.R. Chen, P.J. Chen, Effects of coarse aggregates on the electrical resistivity of Portland cement concrete, Constr. Build. Mater. 133 (2017) 397–408. https://doi.org/10.1016/j.conbuildmat.2016.12.044.

[22] A. Belli, A. Mobili, T. Bellezze, F. Tittarelli, P. Cachim, Evaluating the self-sensing ability of cement mortars manufactured with graphene nanoplatelets, virgin or recycled carbon fibers through piezoresistivity tests, Sustain. 10 (2018). https://doi.org/10.3390/su10114013.

[23] B. Han, X. Guan, J. Ou, Electrode design, measuring method and data acquisition system of carbon fiber cement paste piezoresistive sensors, Sensors Actuators, A Phys. 135 (2007) 360–369. https://doi.org/10.1016/j.sna.2006.08.003.

[24] R.M. Ferreira, S. Jalali, NDT measurements for the prediction of 28-day compressive strength, NDT E Int. 43 (2010) 55–61. https://doi.org/10.1016/j.ndteint.2009.09.003.

[25] A.Q. Nguyen, G. Klysz, F. Deby, J.P. Balayssac, Assessment of the electrochemical state of steel reinforcement in water saturated concrete by resistivity measurement, Constr. Build. Mater. 171 (2018) 455–466. https://doi.org/10.1016/j.conbuildmat.2018.01.155.

[26] R. Kurda, J. de Brito, J.D. Silvestre, Water absorption and electrical resistivity of concrete with recycled concrete aggregates and fly ash, Cem. Concr. Compos. 95 (2019) 169–182. https://doi.org/10.1016/j.cemconcomp.2018.10.004.

[27] W. Morris, A. Vico, M. Vazquez, S.R. De Sanchez, Corrosion of reinforcing steel evaluated by means of concrete resistivity measurements, Corros. Sci. 44 (2002) 81–99. https://doi.org/10.1016/S0010-938X(01)00033-6.

[28] C. Alonso, C. Andrade, J.A. González, Relation between resistivity and corrosion rate of reinforcements in carbonated mortar made with several cement types, Cem. Concr. Res. 18 (1988) 687–698. https://doi.org/10.1016/0008-8846(88)90091-9.

[29] K. Hornbostel, C.K. Larsen, M.R. Geiker, Relationship between concrete resistivity and

corrosion rate - A literature review, Cem. Concr. Compos. 39 (2013) 60–72. https://doi.org/10.1016/j.cemconcomp.2013.03.019.

[30] J.F. Lataste, C. Sirieix, D. Breysse, M. Frappa, Electrical resistivity measurement applied to cracking assessment on reinforced concrete structures in civil engineering, NDT E Int. 36 (2003) 383–394. https://doi.org/10.1016/S0963-8695(03)00013-6.

[31] N. Wiwattanachang, P.H. Giao, Monitoring crack development in fiber concrete beam by using electrical resistivity imaging, J. Appl. Geophys. 75 (2011) 294–304. https://doi.org/10.1016/j.jappgeo.2011.06.009.

[32] R. Ranade, J. Zhang, J.P. Lynch, V.C. Li, Influence of micro-cracking on the composite resistivity of Engineered Cementitious Composites, Cem. Concr. Res. 58 (2014) 1–12. https://doi.org/10.1016/j.cemconres.2014.01.002.

[33] J. Tanesi, A. Ardani, Surface Resistivity Test Evaluation as an Indicator of the Chloride Permeability of Concrete, TechBrief. (2012) 1–6. https://doi.org/10.1159/000112919.

[34] O. Sengul, O.E. Gjørv, Electrical resistivity measurements for quality control during concrete construction, ACI Mater. J. 105 (2008) 541–547. https://doi.org/10.14359/20195.

[35] K.R. Backe, O.B. Lile, S.K. Lyomov, Characterizing curing cement slurries by electrical conductivity, SPE Drill. Complet. 16 (2001) 201–207. https://doi.org/10.2118/74694-pa.

[36] X. Dérobert, J.F. Lataste, J.P. Balayssac, S. Laurens, Evaluation of chloride contamination in concrete using electromagnetic non-destructive testing methods, NDT E Int. 89 (2017) 19–29. https://doi.org/10.1016/j.ndteint.2017.03.006.

[37] S.E.S. Mendes, R.L.N. Oliveira, C. Cremonez, E. Pereira, E. Pereira, R.A. Medeiros-Junior, Electrical resistivity as a durability parameter for concrete design: Experimental data versus estimation by mathematical model, Constr. Build. Mater. 192 (2018) 610–620. https://doi.org/10.1016/j.conbuildmat.2018.10.145.

[38] S.J. Kwon, M.Q. Feng, S.S. Park, Characterization of electromagnetic properties for durability performance and saturation in hardened cement mortar, NDT E Int. 43 (2010) 86–

95. https://doi.org/10.1016/j.ndteint.2009.09.002.

[39] Y. Huang, H. Li, S. Qian, Self-sensing properties of Engineered Cementitious Composites, Constr. Build. Mater. 174 (2018) 253–262. https://doi.org/10.1016/j.conbuildmat.2018.04.129.

[40] O. Sengul, Factors affecting the electrical resistivity of concrete, RILEM Bookseries. 6 (2012) 263–269. https://doi.org/10.1007/978-94-007-0723-8_38.

[41] F. Presuel-Moreno, Y.Y. Wu, Y. Liu, Effect of curing regime on concrete resistivity and aging factor over time, Constr. Build. Mater. 48 (2013) 874–882. https://doi.org/10.1016/j.conbuildmat.2013.07.094.

[42] H. Layssi, P. Ghods, A.R. Alizadeh, M. Salehi, Electrical Resistivity of Concrete Concepts, applications, and measurement techniques, n.d.

[43] C.G. Berrocal, K. Hornbostel, M.R. Geiker, I. Löfgren, K. Lundgren, D.G. Bekas, Electrical resistivity measurements in steel fibre reinforced cementitious materials, Cem. Concr. Compos. 89 (2018) 216–229. https://doi.org/10.1016/j.cemconcomp.2018.03.015.

[44] A. Al-Dahawi, M.H. Sarwary, O. Öztürk, G. Yildirim, A. Akin, M. Şahmaran, M. Lachemi, Electrical percolation threshold of cementitious composites possessing self-sensing functionality incorporating different carbon-based materials, Smart Mater. Struct. 25 (2016). https://doi.org/10.1088/0964-1726/25/10/105005.

[45] T. Ch Madhavi, S. Annamalai, ELECTRICAL CONDUCTIVITY OF CONCRETE, 11 (2016). www.arpnjournals.com (accessed January 16, 2020).

[46] A. Belli, A. Mobili, T. Bellezze, F. Tittarelli, Commercial and recycled carbon/steel fibers for fiber-reinforced cement mortars with high electrical conductivity, Cem. Concr. Compos. (2020) 103569.

[47] R.B. Polder, W.H.A. Peelen, Characterisation of chloride transport and reinforcement corrosion in concrete under cyclic wetting and drying by electrical resistivity, Cem. Concr. Compos. 24 (2002) 427–435. https://doi.org/10.1016/S0958-9465(01)00074-9.

[48] R.M. Andrew, Global CO_2 emissions from cement production, Earth Syst. Sci. Data. 10 (2018) 195–217. https://doi.org/10.5194/essd-10-195-2018.

[49] Home | Endurcrete, (n.d.). http://www.endurcrete.eu/ (accessed March 2, 2020).

[50] EN 197-1:2011 Cement - Part 1: Composition, specifications and conformity criteria for common cements, (n.d.). http://store.uni.com/catalogo/en-197-1-2011?josso_back_to=http://store.uni.com/josso-security-check.php&josso_cmd=login_optional&josso_partnerapp_host=store.uni.com (accessed March 12, 2020).

[51] G. Bolte, M. Zajac, J. Skocek, M. Ben Haha, Development of composite cements characterized by low environmental footprint, J. Clean. Prod. 226 (2019) 503–514. https://doi.org/10.1016/j.jclepro.2019.04.050.

[52] EN 15801 Conservation of cultural property - Test methods - Determination of water absorption by capillarity, n.d. http://store.uni.com/catalogo/index.php/en-15801-2009?josso_back_to=http://store.uni.com/josso-security-check.php&josso_cmd=login_optional&josso_partnerapp_host=store.uni.com.

[53] UNI EN ISO 9227 Corrosion tests in artificial atmospheres — Salt spray tests, n.d. http://store.uni.com/catalogo/index.php/uni-en-iso-9227-2017.

[54] F. Tittarelli, A. Mobili, C. Giosuè, A. Belli, T. Bellezze, Corrosion behaviour of bare and galvanized steel in geopolymer and Ordinary Portland Cement based mortars with the same strength class exposed to chlorides, Corros. Sci. 134 (2018) 64–77. https://doi.org/10.1016/j.corsci.2018.02.014.

[55] UNI 9944 Corrosion and protection of steel in concrete. Determination of the carbonation depth and of the profile of chloride ions penetration in cocrete, n.d. http://store.uni.com/catalogo/index.php/uni-9944-1992.

[56] A.A. Ramezanianpour, A. Pilvar, M. Mahdikhani, F. Moodi, Practical evaluation of relationship between concrete resistivity, water penetration, rapid chloride penetration and

compressive strength, Constr. Build. Mater. (2011). https://doi.org/10.1016/j.conbuildmat.2010.11.069.

[57] J. Silva, J. de Brito, R. Veiga, Incorporation of fine ceramics in mortars, Constr. Build. Mater. 23 (2009) 556–564. https://doi.org/10.1016/j.conbuildmat.2007.10.014.

[58] Y. Benachour, C.A. Davy, F. Skoczylas, H. Houari, Effect of a high calcite filler addition upon microstructural, mechanical, shrinkage and transport properties of a mortar, Cem. Concr. Res. 38 (2008) 727–736. https://doi.org/10.1016/j.cemconres.2008.02.007.

[59] O.R. Ogirigbo, L. Black, Chloride binding and diffusion in slag blends: Influence of slag composition and temperature, Constr. Build. Mater. 149 (2017) 816–825. https://doi.org/10.1016/j.conbuildmat.2017.05.184.

[60] K. De Weerdt, D. Orsáková, A.C.A. Müller, C.K. Larsen, B. Pedersen, M.R. Geiker, Towards the understanding of chloride profiles in marine exposed concrete, impact of leaching and moisture content, Constr. Build. Mater. 120 (2016) 418–431. https://doi.org/10.1016/j.conbuildmat.2016.05.069.

[61] K. De Weerdt, B. Lothenbach, M.R. Geiker, Comparing chloride ingress from seawater and NaCl solution in Portland cement mortar, Cem. Concr. Res. 115 (2019) 80–89. https://doi.org/10.1016/j.cemconres.2018.09.014.